NeuroImage: Clinical 32 (2021) 102798

Contents lists available at ScienceDirect

NeuroImage: Clinical

journal homepage: www.elsevier.com/locate/ynicl

Standardizing T1-w/T2-w ratio images in trigeminal neuralgia to estimate the degree of demyelination *in vivo*

Cathy Meng Fei Li [a,b,c,1], Powell P.W. Chu [b,1], Peter Shih-Ping Hung [b,c,d], David Mikulis [c], Mojgan Hodaie [b,c,d,*]

[a] Department of Clinical Neurological Sciences, University of Western Ontario, Ontario, Canada
[b] Division of Neurosurgery, Department of Surgery, Toronto Western Hospital, University Health Network, University of Toronto, Toronto, Ontario, Canada
[c] Division of Brain, Imaging, and Behavior – Systems Neuroscience, Krembil Research Institute, Toronto Western Hospital, University Health Network, Toronto, Ontario, Canada
[d] Institute of Medical Science, University of Toronto, Toronto, Ontario, Canada

ARTICLE INFO

Keywords:
Neuroimaging
Myelin
T1-w/T2-w ratio
Trigeminal neuralgia

ABSTRACT

Background: Novel magnetic resonance (MR) imaging techniques have led to the development of T1-w/T2-w ratio images or "myelin-sensitive maps (MMs)" to estimate and compare myelin content *in vivo*. Currently, raw image intensities in conventional MR images are unstandardized, preventing meaningful quantitative comparisons. We propose an improved workflow to standardize the MMs, which was applied to patients with classic trigeminal neuralgia (CTN) and trigeminal neuralgia secondary to multiple sclerosis (MSTN), to assess the validity and feasibility of this clinical tool.

Methods: T1-w and T2-w images were obtained for 17 CTN patients and 17 MSTN patients using a 3 T scanner. Template images were obtained from ICBM152. Multiple sclerosis (MS) plaques in the pons were labelled in MSTN patients. For each patient image, a Gaussian curve was fitted to the histogram of its intensity distribution, and transformed to match the Gaussian curve of its template image.

Results: After standardization, the structural contrast of the patient image and its histogram more closely resembled the ICBM152 template. Moreover, there was reduced variability in the histogram peaks of the gray and white matter between patients after standardization ($p < 0.001$). MM intensities were decreased within MS plaques, compared to normal-appearing white matter (NAWM) in MSTN patients ($p < 0.001$) and its corresponding regions in CTN patients ($p < 0.001$).

Conclusions: Images intensities are calibrated according to a mathematic relationship between the intensities of the patient image and its template. Reduced variability among histogram peaks allows for interpretation of tissue-specific intensity and facilitates quantitative analysis. The resultant MMs facilitate comparisons of myelin content between different regions of the brain and between different patients *in vivo*. MM analysis revealed reduced myelin content in MS plaques compared to its corresponding regions in CTN patients and its surrounding NAWM in MSTN patients. Thus, the standardized MM serves as a non-invasive, easily-automated tool that can be feasibly applied to clinical populations for quantitative analyses of myelin content.

1. Introduction

Novel magnetic resonance (MR) imaging techniques can provide valuable information about gray matter (GM) and white matter (WM) of the brain. Different MR sequences vary in their sensitivity to certain intracranial processes and pathologies, such as multiple sclerosis (MS), microangiopathic disease, and stroke (Halefoglu and Yousem, 2018; Kilburg et al., 2017; Inglese and Petracca, 2018). However, conventional MR sequences do not provide sufficient information on the state of myelin and T1-w/T2-w ratio images were developed to address this

Abbreviations: CIS, clinically isolated syndrome; RR, relapse-remitting; Prog, progressive (including primary and secondary progressive MS); SD, standard deviation.

* Corresponding author at: Toronto Western Hospital, Division of Neurosurgery, 399 Bathurst Street, 4W W-443, Toronto, Ontario M5T 2S8.
E-mail address: mojgan.hodaie@uhn.ca (M. Hodaie).

[1] Cathy Meng Fei Li and Powell P.W. Chu are first co-authors on this manuscript.

https://doi.org/10.1016/j.nicl.2021.102798
Received 4 May 2021; Received in revised form 4 July 2021; Accepted 17 August 2021
Available online 21 August 2021

limitation (Glasser and Van Essen, 2011; Ganzetti et al., 2014; Gordon et al., Oct. 2019). The T1-w/T2-w ratio image is a non-invasive, clinically-derived tool that capitalizes on conventional MR sequences to quantify myelin, and has the potential to serve as a valuable adjunctive tool in assessing patients with neurological or demyelinating diseases.

Myelin sheath is the dominant source of WM contrast in MR imaging and typically appears hyperintense relative to GM on T1-w images (Halefoglu and Yousem, 2018; Kilburg et al., 2017). On the other hand, the hydrophobic property of the lipidic bilayer in myelin restricts the molecular motion of protons, causing myelin to appear hypointense on T2-w images (Barkovich, 2000; Koenig, 1991). By dividing their raw image intensities, the T1-w/T2-w ratio effectively increases the contrast-to-noise ratio, and thereby, produces myelin-enhanced contrast images (Schiffmann, 2009).

One of the challenges of using conventional MR sequences to measure myelin is that the raw image intensity vary as a result of acquisition protocols, physical scanners, and subject-related factors, thus rendering these measurements meaningless (Roy et al., 2013; Shinohara et al., 2014; Clark et al., 2006; Fang et al., 2005). To address the inconsistencies of these acquisition factors, Glasser et al. (Glasser and Van Essen, 2011) used an internal calibration method, where cortical regions were parcellated and calibrated based on the putative myelocytoarchitectural map of the brain (Fischl et al., 2004). Glasser's method illustrated the full spectrum of myelination within the brain, from the lightly-myelinated anterior insula to the heavily-myelinated motor cortex. Later, Ganzetti et al. (Ganzetti et al., 2014) developed an external calibration method that finessed the contrasting intensities of two non-brain regions (e.g. eyeball and temporalis muscle). Ganzetti's method offered the opportunity for inter-subject comparisons, but the resultant T1-w/T2-w maps remain dependent on acquisition factors, thereby limiting the generalization of this technique (Hagiwara et al., 2018; Uddin et al., 2017). Previous work by Nyul and Udupa (Nyul and Udupa, 1999) integrated a histogram matching algorithm to normalize the intensity scale for MR image display. This technique is independent of acquisition factors (Shah et al., 2011), but has yet to be explored in the context of constructing standardized T1-w/T2-w ratio images.

In our study, we propose an improved workflow to generate T1-w/T2-w ratio maps that allow inter-subject comparison, while eliminating the need for tissue- and sequence-dependent standardization. We apply the revised T1-w/T2-w ratio maps to the pontine region of the brainstem, a typically myelin-rich component of the central nervous system, to study its changes in two clinically-similar populations. Specifically, we compare the MMs of patients with classic trigeminal neuralgia (CTN) and patients with trigeminal neuralgia secondary to multiple sclerosis (MSTN). Although both clinical populations present with lancinating facial pain, the etiology of their pain is different. MS plaques in the brainstem are theorized to produce ephaptic transmission of pain in MSTN patients (Fischl et al., 2004; Hagiwara et al., 2018), whereas the etiology of CTN is largely due to compression of the trigeminal nerve by a neighbouring blood vessel.

In the context of demyelinating diseases such as MS, the revised T1-w/T2-w ratio map serves as a surrogate marker of myelin content and henceforth will be referred to as a "myelin-sensitive map (MM)". By applying MMs to these two patient populations, this study aims to develop a MM workflow that maximizes its generalizability and feasibility, and to demonstrate the clinical application of MMs in estimating myelin damage *in vivo*. We hypothesize that MM analysis will demonstrate reduced myelin content in MS plaques compared to corresponding WM regions in CTN patients and normal-appearing white matter (NAWM) in MSTN patients.

2. Methods

2.1. Participant and study design

This is a retrospective study comprised of 34 patients, where 17 patients were diagnosed with CTN and 17 patients were diagnosed with MSTN. At least one neuroradiologist and one neurosurgeon have reviewed the MR images to appropriately classify patients as CTN and MSTN. The diagnoses of CTN meet the criteria outlined in the International Classification of Headache Disorders (Olesen, 2018) and the diagnoses of MS are consistent with the 2017 Revised McDonald Criteria (Thompson et al., 2018). In brief, the inclusion criteria were patients with 1) neuropathic facial pain involving one or more branches of the trigeminal nerve whose diagnoses are consistent with CTN or MSTN, 2) no prior surgeries or procedures for their CTN or MSTN pain, and 3) standard MR images available as described below. CTN patients with comorbidities in the central nervous system (CNS) were excluded from the study; MSTN patients with non-MS comorbidities in the CNS were similarly excluded. MR images with temporarily-enlarged perivascular spaces (PVS) were also excluded, as these spaces may be temporarily enlarged (>2mm in diameter) in healthy individuals and their clinical significance remain uncertain (Maclullich et al., 2004). Table 1 shows the demographics of all 34 patients. The two groups were matched by sex and age (±4 years). The study was approved by the Research Ethics Board.

2.2. Image acquisition

Magnetic resonance (MR) images were acquired using a GE Signa HDx 3 T scanner with an eight-channel head coil. For this study, 3D fast spoiled gradient echo (FSPGR) T1-w anatomical images and 3D fast imaging employing steady-state acquisition (FIESTA) T2-w anatomical images were obtained for each patient. All MR images were anonymized.

T1-w FSPGR images were acquired with an in-plane resolution of 0.9375×0.9375 mm, slice thickness = 1 mm, echo time (TE) = 5.052 ms, repetition time (TR) = 11.956 ms, inversion time (TI) = 300 ms, flip angle = 20°, field of view (FOV) = 240 mm, and matrix = 256×256. The scan time for T1-w FSPGR images was 7.3 min. The number of slices ranged from 124 to 180 depending on the patient's head size. The default setting for T1-w FSPGR is 146 slices, which was obtained in 44% of patients. Approximately 18% of patients had less than 146 slices, and 38% had more than 146 slices.

T2-w FIESTA images were acquired with an in-plane resolution of 0.4297×0.4297 mm, slice thickness = 4 mm, TE = 94.14 ms, TR = 5200 ms, flip angle = 90°, FOV = 170 mm, and matrix = 512×512. The scan time for T2-w FIESTA images was 6.1 min. The number of slices ranged from 64 to 116 slices depending on the patient's head size. The default setting for T2-w FIESTA images is 76 slices (obtained in 47% of patients) or 84 slices (obtained in 41% of patients). Approximately 6% of patients had less than 76 slices, and 9% had more than 84 slices.

FLAIR images were acquired with an in-plane resolution of 0.4297×0.4297 mm, slice thickness = 4 mm, TE = 141.4 ms, TR = 8652 ms, flip angle = 90°, FOV = 220 mm, and matrix = 384×224. The scan time for FLAIR images was 5.8 min. FLAIR images were used to verify the presence of MS plaques.

2.3. Image processing

The pipeline of the study, shown in Fig. 1, is modified from Ganzetti et al. (Ganzetti et al., 2014). Briefly, all T1-w and T2-w images were bias corrected for radiofrequency field inhomogeneities using FSL's FAST (Zhang et al., 2001). The skull and other non-brain tissues were removed using the Brain Extraction (BET2) package in FSL 5.0 (FMRIB Software Library, www.fmrib.ox.ac.uk/fsl/). All T1-w and T2-w images were then resampled to yield identical voxel sizes of 0.9375×0.9375×1 mm using 3D Slicer version 4.3 (NA-MIC©, http://www.slicer.org). As part of the co-registration process, each T2-w image undergoes a rigid body transformation to its respective T1-w image using the Advanced Normalization Tools (ANTs, http://stnava.github.io/ANTs/) (Avants et al., 2011).

Table 1
Demographics of the MSTN and CTN groups.

CTN Subject ID	Sex	Age (years old)	Duration of TN (years)	MSTN Subject ID	Sex	Age (years old)	Duration of MS (years)	Duration of TN (years)	Type of MS
CTN43	F	55	2	01	F	51	8	1	Prog.
CTN28	F	40	8	02	F	44	14	0	RR
CTN16	F	45	3	03	F	44	23	11	RR
CTN37	M	46	8	04	M	49	9	0	RR
CTN30	M	59	12	06	M	63	45	3	RR
CTN27	F	49	2	08	F	49	8	8	Prog.
CTN20	F	47	2	09	F	45	19	4	RR
CTN08	F	54	4	12	M	51	29	10	Prog.
CTN45	M	31	2	13	F	31	1	1	CIS
CTN38	F	46	5	14	F	44	6	6	RR
CTN31	F	67	0.9	15	F	67	0	10	RR
CTN03	F	69	10	16	F	68	27	3	Prog.
CTN05	F	58	3	18	F	58	30	4	RR
CTN17	F	51	10	19	F	50	10	0	RR
CTN47	M	44	1	20	M	47	8	N/A	RR
CTN06	F	38	6	21	F	36	11	2	RR
CTN12	M	52	6	22	M	52	30	3	Prog.
Mean (±SD)	12F: 5 M	50.06 ± 9.85	4.99 ± 3.51	Mean (±SD)	12F: 5 M	49.94 ± 9.85	16.35 ± 12.41	4.13 ± 3.77	

CTN and MSTN patients were age- and sex-matched (N = 34). Of the seventeen MSTN patients, 11 had relapse-remitting MS, 5 had a progressive form of MS, and 1 presented with trigeminal neuralgia as a clinically isolated syndrome prior to her diagnosis of multiple sclerosis. There was no significant difference between duration of TN between CTN and MSTN patients. Progressive forms of MS include both primary and secondary progressive MS. There was one MSTN patient (Subject 20) that did not have any clinical documentation stating onset of TN.
Abbreviations: CIS = clinically isolated syndrome, RR = relapse-remitting, Prog. = progressive (including primary and secondary progressive MS).

2.4. Image standardization

The standardization process is adapted from a histogram matching algorithm described in Nyul and Udupa (Nyul and Udupa, 1999), where the T1-w and T2-w images are calibrated according to the relationship between the intensity distributions of a particular image and its corresponding template image.

T1-w and T2-w images from the ICBM 2009c Nonlinear Asymmetric atlas (NIFTI) were used as template images (http://www.bic.mni.mcgill.ca/ServicesAtlases/ICBM152NLin2009) (Fonov et al., 2009; Fonov et al., 2011), and represent MR images for the healthy population. For each template image, the intensity distribution of the entire post-processed brain volume was obtained (bins = 15001). A Gaussian curve fit was performed on the intensity distribution of each image using the parameters as defined by the *curve_fit* function in SciPy (a Python library for scientific computing). The minimum and maximum image intensities of the Gaussian curve were computed to ensure that 99% of the voxel intensities fell within this interval.

The histograms of the T1-w and T2-w image intensities were obtained separately for all patients. For each histogram, a Gaussian curve fit was performed in an identical process as described above for the template images. To standardize the histograms of the image intensities, the Gaussian-fitted curve of each patient's image was transformed to match the Gaussian-fitted curve of its respective template image, in accordance to the following formula:

$$\tau(x) = \begin{cases} \mu_s + (x - \mu_p)\dfrac{s_1 - \mu_s}{p_1 - \mu_p}, & if\ x \leqslant \mu_p \\ \mu_s + (x - \mu_p)\dfrac{s_2 - \mu_s}{p_2 - \mu_p}, & if\ x \geqslant \mu_p \end{cases} \quad (1)$$

where

x = original voxel intensity of the patient's image
μ_s = intensity of the template where the Gaussian curve is at its peak
s_1 = minimum intensity of the Gaussian curve for the template
s_2 = maximum intensity of the Gaussian curve for the template
μ_p = intensity of the patient's image where the Gaussian curve is at its peak
p_1 = minimum intensity of the Gaussian curve for the patient's image
p_2 = maximum intensity of the Gaussian curve for the patient's image

The standardization protocol established the three landmarks (μ_p, p_1, and p_2) from each Gaussian curve to transform its corresponding histogram. The goal of the transformation was to match the peak (μ_p) and interval (p_1 to p_2) of the patient's image to the peak (μ_s) and reference interval (s_1 to s_2) of its respective template image (Fig. 2). For each of the 34 patients, a separate transformation was performed for T1-w and T2-w images.

Using the co-registered images and the standardized intensity distributions, the T1-w image intensities are divided by T2-w image intensities and the resultant standardized T1-w/T2-w ratio map or MM is created in the patient's native T1 space. The MM intensities serve as a surrogate marker of the myelination level. All MMs were nonlinearly transformed into the ICBM152 T1 template space using ANTs. Fig. 3 illustrates the MMs of the pontine region for one CTN patient and one MSTN patient.

2.5. Image analysis: Gray and white matter

The GM and WM images of the ICBM152 template were downloaded from the ICBM 2009c Nonlinear Asymmetric atlas. Binary masks for the GM and WM were created using an intensity threshold = 0.5 in FSL. The masks were applied to the ICBM152 T1 and T2 template images, and a Gaussian curve fit was performed for each set of intensity values. The boundaries and peaks of the Gaussian curves were determined using FSL.

Both GM and WM masks underwent nonlinear transformation from ICBM152 T1 template space to patient's native T1 space, and subsequent linear transformation to the patient's native T2 space. A Gaussian curve fit was performed to obtain the mean intensity of the GM and WM for all standardized T1-w images; this was repeated for all standardized T2-w images.

2.6. Image analysis: MS plaques

For each MSTN patient, MS plaques were manually identified as areas of hypointensities on T1-w images and hyperintensities on T2-w images in the pontine regions. FLAIR images were used to confirm the MS plaques.

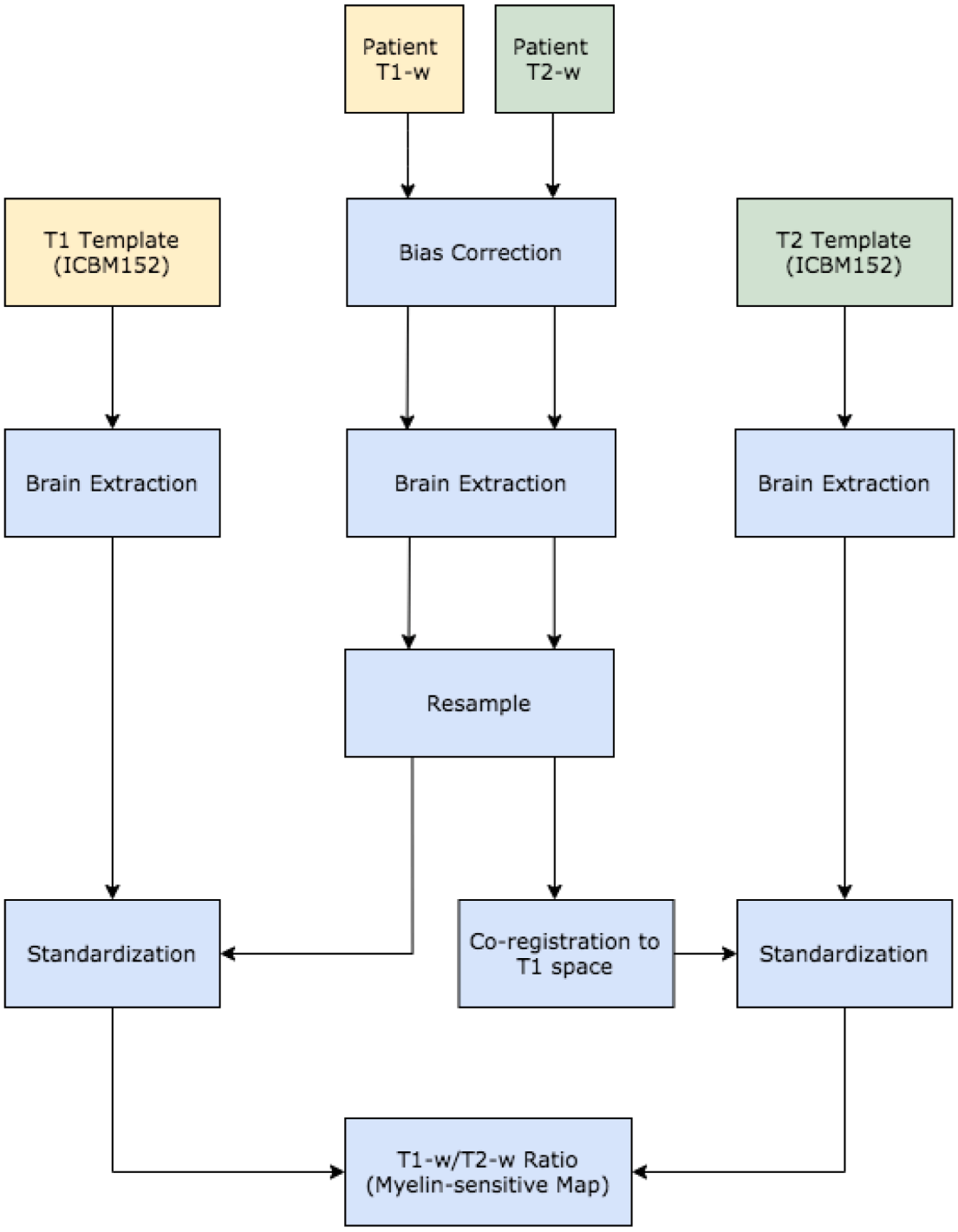

Fig. 1. Diagram of the MM workflow. All T1-w and T2-w images were bias corrected and brain extracted. The subsequent images were resampled and standardized to their respective ICBM152 template images (Fonov et al., 2009; Fonov et al., 2011). The ratio of the bias-corrected and standardized T1-w and T2-w images was calculated for each patient to obtain the MM, which can then be used to estimate myelin content.

Version 4.3 of 3D Slicer was used to create two regions of interest (ROIs) in the patient's native T1-w space: 1) pontine regions with MS plaques were designated as "plaqueROI", and 2) pontine regions without MS plaques were designated as "noplaqueROI". All ROIs underwent nonlinear transformation from the patient's native T1 space to the ICBM152 T1 template space. The transformed "plaqueROIs" and "noplaqueROIs" were applied to the MMs in ICBM152 T1 template space for subsequent quantitative analysis (Fig. 4). A Gaussian curve fit was performed to obtain the mean MM intensity within the ROIs for CTN and MSTN patients.

2.7. Statistical analysis

Statistical analysis was performed using the R software suite. Pearson's correlation coefficient was used to determine statistical significance of correlations.

The coefficient of variation (CV) was calculated to determine the variability in voxel intensity of the GM and WM peaks among all patients. The CVs were calculated for T1-w and T2-w sequences at two time-points (before and after standardization). A two-sample *t*-test was conducted to compare differences in CVs before and after

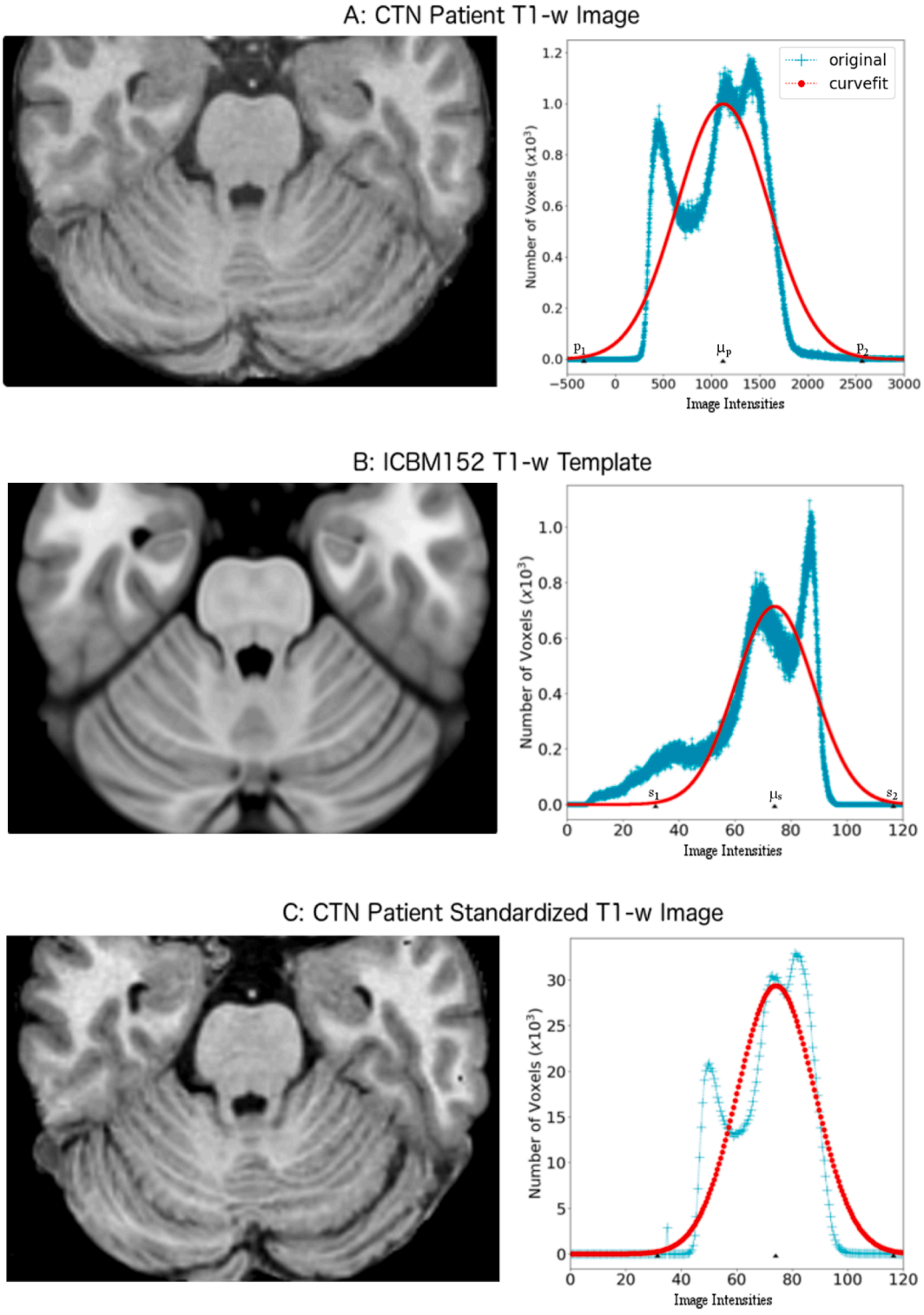

Fig. 2. Standardizing the T1-w image intensities using Gaussian curve-fit. Panel A illustrates the original T1-w image of a CTN patient and its intensity distribution. The teal blue marker, labelled as "original", represents the raw histogram of the image intensities. The red marker, labelled as "curvefit", represents the Gaussian curve fit of the histogram. The three landmarks (p_1, p_2, and μ_p) are labelled on the histogram, where μ_p is the image intensity where the Gaussian curve reaches its peak, and p_1 and p_2 define the range of the Gaussian curve within which 99% of image intensities fall. The image intensities of p_1 and p_2 serve as the lower and upper limits of the viewing window for the original T1-w image, respectively. (For interpretation of the references to colour in this figure legend, the reader is referred to the web version of this article.)

standardization.

To assess the internal validity, a two-sample *t*-test was conducted to evaluate differences in MM intensities between the plaqueROI and noplaqueROI regions; this was conducted separately in MSTN and CTN patients.

To assess the clinical utility of MMs in comparing different clinical populations, a two-sample *t*-test was conducted to evaluate differences in the MM intensities between matched CTN and MSTN patients for each

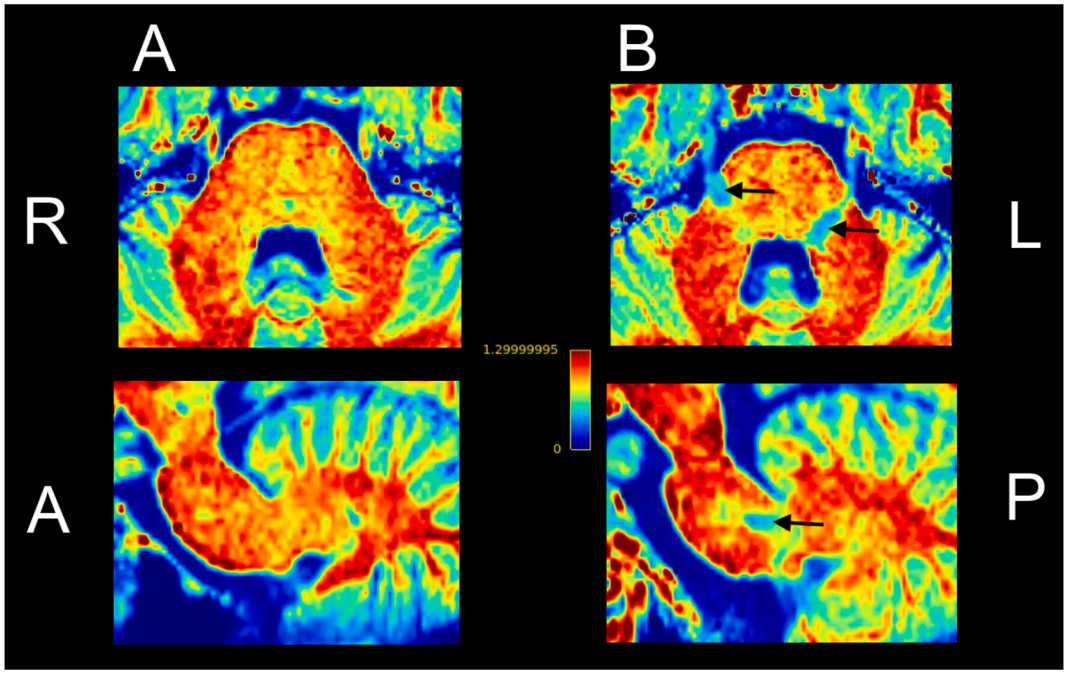

Fig. 3. The MMs of one CTN and one MSTN patient. The T1-w and T2-w images are bias-corrected, co-registered, and standardized before the MM is computed. The colour scale of MM is graded from 0 to 1.3, where 0 suggests least myelinated and 1.3 suggests most myelinated. Panel A demonstrates the axial (top) and sagittal views (bottom) of one CTN patient. Panel B demonstrates the axial (top) and sagittal views (bottom) of one MSTN patient. The axial view illustrates two distinct pontine regions with visibly decreased MM intensities in this MSTN patient (see black arrows).

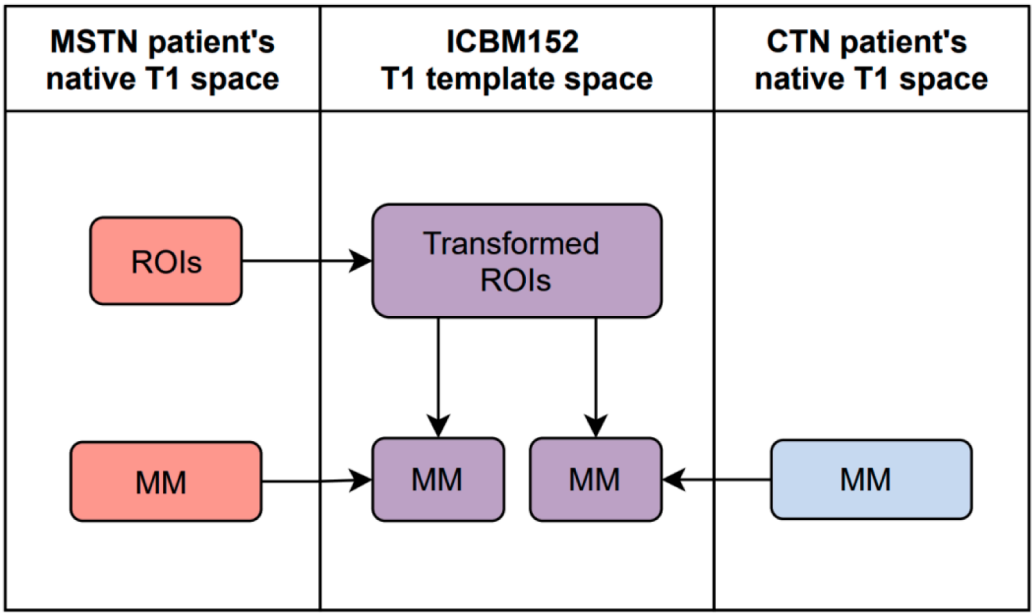

Fig. 4. Application of ROIs onto MMs. In MSTN patients, pontine regions are labelled "plaqueROIs" and "noplaqueROIs" depending on the presence or absence of MS plaques, respectively. The ROIs and MMs undergo nonlinear transformation into the ICBM152 T1 template space using ANTs. The transformed ROIs are then applied to each MM in the ICBM152 T1 template space.

of the two ROIs. An alpha of 0.05 is considered statistically significant.

3. Results

The study included 34 patients, where the 17 MSTN patients were sex- and age-matched with the 17 CTN patients. In each patient group, there are 12 females and 5 males. Patient demographics include a mean age of 50 ± 9.84 years and TN duration of 4.57 ± 3.61 years among all patients (Table 1).

In the MSTN, there are 11 patients diagnosed with relapse-remitting (RR) subtype, 1 patient with clinically-isolated syndrome (CIS), and 5 patients with a progressive form of MS. The progressive category includes both primary and secondary progressive MS, as the two subtypes are biologically similar. (Ontaneda et al., 2017) Overall, there are no significant differences in demographics between the CTN and MSTN patients (Table 1).

3.1. ICBM152 templates

The ICBM152 T1 template exhibits a bimodal distribution with a reference interval from 31.6 to 116.58 image intensity units. The peaks of the bimodal distribution closely coincide with the peaks of the GM and WM curve fits, which are at 68.30 units and 85.28 units, respectively. The μ_s or the mean intensity of the T1 template is measured at 74.10 units.

The ICBM152 T2 template exhibits a unimodal distribution with a reference interval from 18.26 to 78.03 image intensity units. The peaks of the GM and WM curve fits for the T2 template are at 53.75 units and 42.67 units, respectively. The μ_s of the T2 template is at an intensity of 48.14 units.

3.2. Qualitative analysis

A visual comparison between one patient's pre-standardized T1-w image and its ICBM152 template image demonstrates obvious discrepancies in tissue intensities, where the WM in the template appears relatively hyperintense to the patient's image (Fig. 2). In addition, the histogram of the T1-w template demonstrates a relatively left-skewed distribution, compared to the histogram of the patient's T1-w image (Fig. 2). After standardization, the structural contrast and image intensities of the patient's MR image more closely resemble that of the ICBM152 template. Similarly, the intensity distribution is standardized to the same reference interval as the template to help maintain consistency in the tissue meaning of the image intensities (Fig. 2).

The original histograms of the MR images vary widely between subjects, particularly for T2-w FIESTA images. After standardization, the intensities of the histogram peaks are better aligned with each other (Fig. 5), and this consistency is important for subsequent quantitative analyses. In each cohort (n = 17), there are 34 histograms that are transformed; for example, in MSTN patients, there are 17 T1-w histograms and 17 T2-w histograms that are each transformed to ensure a similar distribution of image intensities as their respective templates (Fig. 5**).**

The MM is computed using the standardized T1-w and T2-w images. A visual analysis of the MM for one CTN and one MSTN patient demonstrates the clear delineations of MS plaques from the remainder of the brain tissues (Fig. 3). In all other regions of the brain, the MM intensities appear consistent between the CTN and MSTN patient. In some MSTN patients, the MMs also demonstrate areas of subtle myelin reduction in the pontine NAWM that were not clinically identified as plaques on the T1-w and T2-w images (Fig. 6).

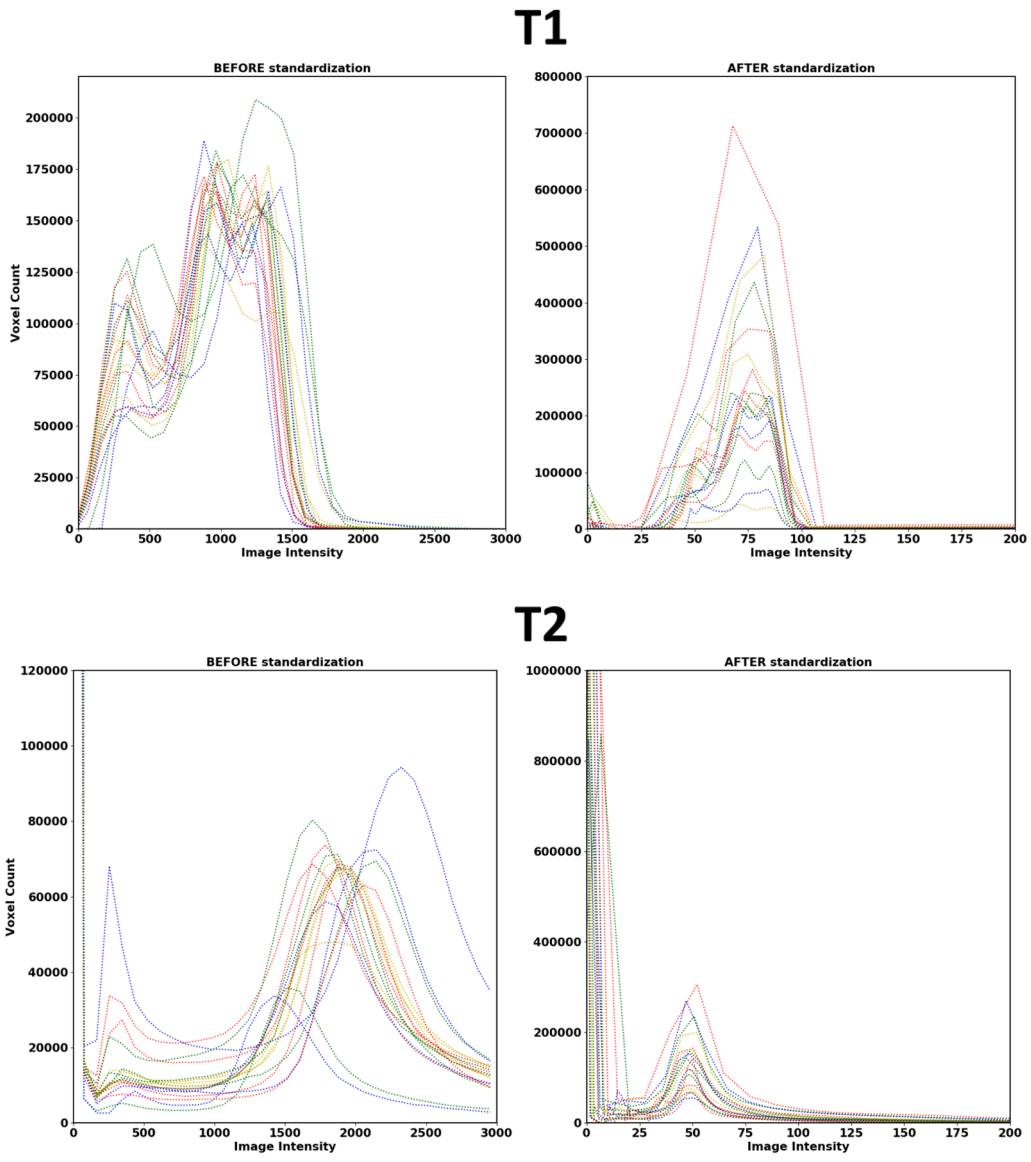

Fig. 5. Standardization using histograms of image intensities in MSTN patients. Panel A shows the histograms of T1-w image intensities before and after standardization. Panel B shows the histogram of T2-w image intensities before and after standardization. In each diagram, each line represents a single subject's intensity distribution across the entire image. The image intensity of each subject's peak frequency is better aligned after standardization. All images are bias-corrected and brain-extracted.

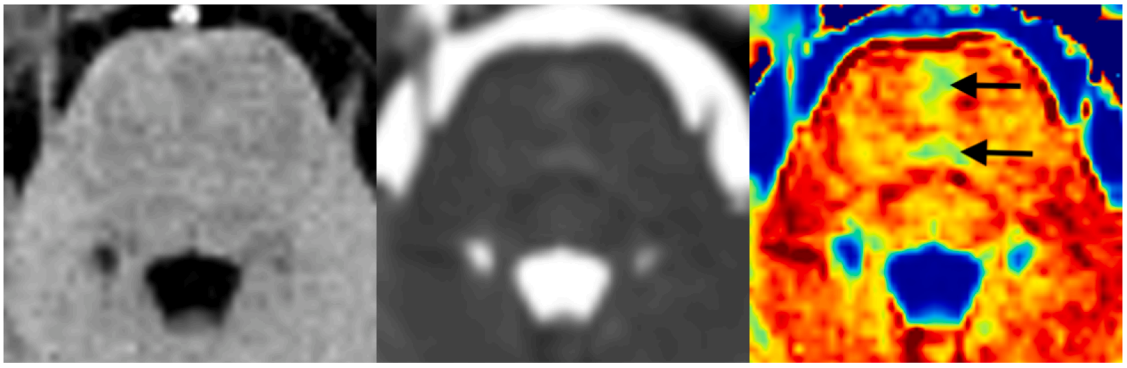

Fig. 6. T1-w FSPGR, T2-w FIESTA, and MM of one MSTN patient. In one MSTN patient who did not have any obvious MS pontine plaques on T1-w and T2-w images, the MM demonstrated two focal areas of reduced myelin content in the pons (see arrows). Although there were some subtle T2 hyperintensities in the pons, these poorly-delineated regions were not clinically identified as plaques on T1-w and T2-w images. Compared to conventional MR images, the MM improved the contrast-to-choice ratio and better demarcated the regions of decreased myelin.

3.3. Standardizing GM and WM

For all pre-standardized T1-w images, the CV for the peaks of GM and WM curve fits are 0.108 and 0.102, respectively. After standardization, the CV for the peaks of GM and WM curve fits are 0.018 and 0.008, respectively (Table 2).

For all pre-standardized T2-w images, the CV for the peaks of GM and WM curve fits are 0.127 and 0.135, respectively. After standardization, the CV for the peaks of GM and WM curve fits are 0.014 and 0.025, respectively (Table 2).

Overall, there was a significant difference in CV before and after standardization ($p < 0.001$). In both T1-w and T2-w images, the standardized peaks demonstrate an approximate a 5-fold to 15-fold reduction in variability compared to pre-standardized peaks.

3.4. Quantitative analysis

In MSTN patients, the difference in MM intensities (mean ± SEM) between noplaqueROIs (1.90 ± 0.01) and plaqueROIs (1.61 ± 0.02) were statistically significant ($p < 0.001$). However, in CTN patients, the MM intensities of the transformed noplaqueROIs (1.88 ± 0.01) and plaqueROIs (1.81 ± 0.03) were not significantly different ($p > 0.05$), as shown in Fig. 7.

Comparing between the two patient populations, MSTN patients had significantly lower MM intensity in the plaqueROIs compared to CTN patients ($p < 0.001$). In the noplaqueROIs, there was no difference in MM intensity between MSTN and CTN patients (Fig. 8**)**.

Within the MSTN cohort, there was no significant difference in MM intensity between patients with progressive MS and those with RRMS or CIS in the plaqueROIs and noplaqueROIs ($p > 0.05$). The MM intensity in the plaqueROIs and noplaqueROIs do not correlate with duration of MS or TN.

Table 2
The coefficient of variation (CV) before and after standardization.

		Coefficient of Variation (CV)	
		Before standardization	After standardization
T1-w	GM	0.108	0.018
	WM	0.102	0.008
T2-w	GM	0.127	0.014
	WM	0.135	0.025
Mean CV		*0.118*	*0.016*
p-value		*<0.001*	

The CV measures the relative dispersion of data around a mean. There is a significant difference in CV before and after standardization ($p < 0.001$). There was at least a 5-fold reduction in CV for all GM and WM peaks in the T1-w and T2-w images.
Abbreviations: GM = gray matter, WM = white matter.

4. Discussion

The standardized T1-w/T2-w ratio images or MMs serve as a reasonably proxy of myelin content in patients with demyelinating diseases such as MS. The MMs facilitate *in vivo* comparisons of myelin content in different regions of the brain and between different patients. MM analysis revealed reduced myelin content in MS plaques compared to their corresponding WM structures in CTN patients and to other pontine regions without obvious plaques in MSTN patients (also known as normal-appearing white matter or NAWM). These findings of reduced myelin content in regions affected by MS pathology are consistent with previous histological studies (Nakamura et al., 2017; Righart et al., 2017). Thus, standardized MMs can allow clinicians to estimate the degree of demyelination in MS plaques *in vivo*, while identifying areas of subtle demyelination prior to plaque formation on conventional MR images.

This novel computational technique builds upon previous calibration methods and exploits the mathematical relationship between the intensities of the patient image and its corresponding template to create standardized MMs (Glasser and Van Essen, 2011; Ganzetti et al., 2014; Uddin et al., 2017). The template image is used as a reference to facilitate both within-patient and across-patient analysis, while ensuring that the workflow is reproducible with similar MR sequences.

To our knowledge, this is the first study to investigate the use of the MMs in comparing two different clinical populations. Patients with MSTN and CTN present with similar symptoms of lancinating facial pain; however, MS plaques may not be apparent until later in the disease process. As such, there is a need to better differentiate between these two patient populations early in their diseases to make appropriate treatment decisions. Further development of MM analysis will permit longitudinal assessment of NAWM in MSTN patients, and correlational studies between the degree of demyelination and onset of MSTN pain.

4.1. Advantages of MMs

The ability to estimate myelin content *in vivo* allows for longitudinal surveillance of NAWM as well as brain regions visibly affected by disease. T1-w and T2-w images are frequently acquired as part of the clinical work-up, and no additional scanning time is required to generate the MMs. Two separate image acquisitions are required to compute the MM, which renders the product relatively robust to motion artifacts. Moreover, there is a high test-retest reliability of MMs (Arshad et al., 2017). This postprocessing technique can be fully automated, which minimizes lag time and allows for real-time analysis in clinical practice. As such, modifying conventional MRI images is a more practical method

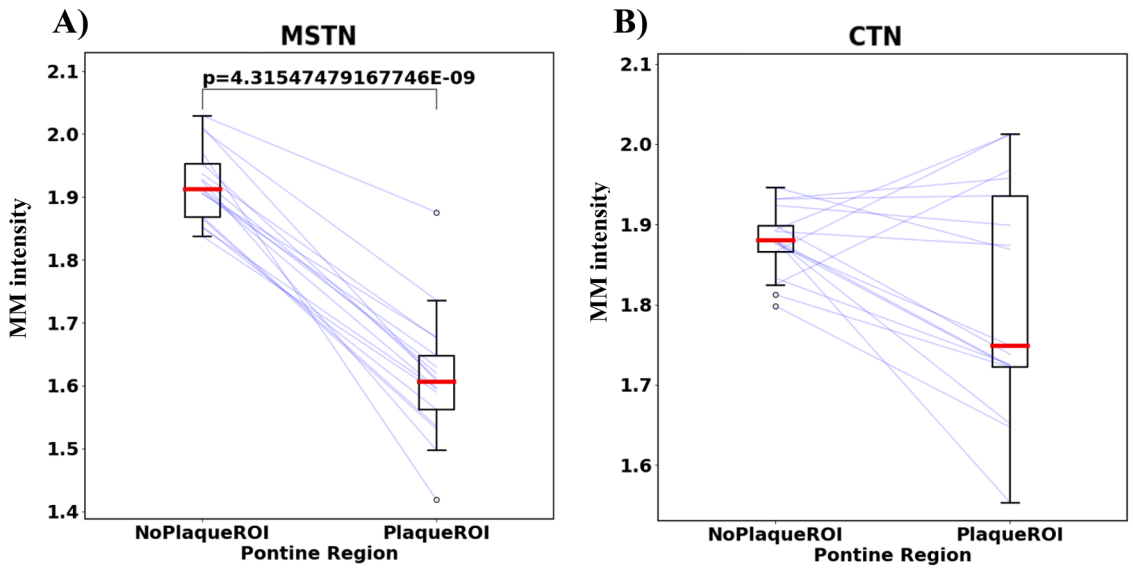

Fig. 7. Quantitative comparison of MM intensity between pontine regions with and without MS plaques in two different clinical populations. In MSTN patients, pontine regions with plaques are labelled as "plaqueROIs" and pontine regions without plaques are labelled as "noplaqueROIs". These same regions were co-registered and compared in CTN patients. In MSTN patients, there is a significant reduction in MM intensity in the plaqueROIs compared to noplaqueROIs ($p < 0.001$). On the other hand, there is no difference in the MM intensity between plaqueROIs and noplaqueROIs in CTN patients ($p > 0.05$).

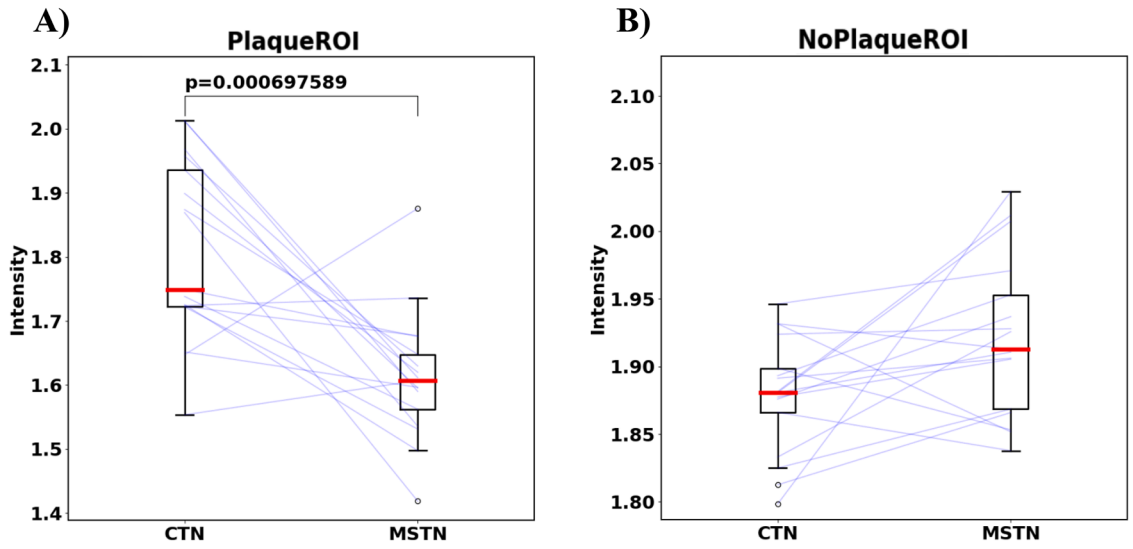

Fig. 8. Quantitative comparison of MM intensity between CTN and MSTN patients in two distinct regions of interests. In MSTN patients, pontine regions with plaques are labelled as "plaqueROIs" and pontine regions without plaques are labelled as "noplaqueROIs". These same regions were labelled in CTN patients. In panel A, there was a significant decrease in the MM intensity of the plaqueROIs in MSTN patients in comparison to CTN patients ($p < 0.001$). In panel B, there is no significant difference in the noplaqueROIs between MSTN and CTN patients ($p > 0.05$).

of estimating myelin content than relying traditional histopathological techniques, which are not always feasible.

4.2. Myelin-sensitive map workflow

Clinical T1-w and T2-w sequences are processed through the workflow, as shown in Fig. 1, to create MMs that facilitate direct comparisons between subjects. Creating a ratio enhances the myelin contrast, given the inverse relationship of myelin's intensity in T1-w and T2-w images. Given the unpredictable variations in MR intensities, a stringent standardization protocol was developed to facilitate meaningful and interpretable comparisons in MM values.

The standardization process in this workflow is based on robust mathematical relationships (Eq. (1)) and uses publicly-available template images as references. Standardization is performed post-hoc, such that special MR sequences and acquisition protocols are not required. This mathematical formula can be broadly applied to various clinical MR sequences (Nyul and Udupa, 1999). This robust standardization process does not rely on non-brain regions, and successfully preserves the relationships between brain-specific tissue intensities (Glasser and Van Essen, 2011; Ganzetti et al., 2014).

In accordance to the protocol described by Nyul and Udupa, we have assigned a reference interval to facilitate standardization of image intensities. The lower (s_1) and upper (s_2) boundaries of the reference interval are based on the publicly-available ICBM152 T1 and T2 templates, allowing this methodology to be easily reproducible and widely-accessible. The reference intervals permit meaningful comparisons between standardized image intensities and across different

subjects. We also used μ_s as a histogram landmark for transformations. The intensity at which the Gaussian curve reaches its peak is also the mode, median, and mode of the Gaussian curve, which effectively accounts for the relative distribution of the image intensities. As such, this standardization process can be employed in unimodal (as seen in T2-w FIESTA images), and bimodal (as seen in T1-w FSPGR images) intensity distributions. After standardization, there is a reduction in variability of GM and WM peaks between patients. The improved consistency in the GM and WM peaks offers tissue-specific intensity information, and sets the foundation for quantitative analysis. Fig. 3 demonstrates that the resultant MMs are consistent with previous T1-w/T2-w ratio maps available in the literature (Glasser and Van Essen, 2011; Ganzetti et al., 2014).

4.3. Comparison between clinical populations

This method can help to facilitate intra-patient and inter-patient comparisons in myelin content. In our study, we applied the MM analysis to compare MSTN patients and CTN patients.

In MSTN patients, there is a significant reduction in the MM intensity in MS plaques, compared to the pontine regions without visible plaques. On the other hand, there is no difference in MM intensity between the transformed plaqueROIs and noplaqueROIs in CTN patients, as the WM in both ROIs are expectedly intact. Overall, the MMs demonstrate that regions with MS plaques had reduced myelin content (Fig. 7), which is in keeping with previous MRI-histological studies (Nakamura et al., 2017; Righart et al., 2017).

We also compared myelin content in the central pontine regions between the two clinical populations, which demonstrated that there was no difference in MM intensity between the NAWM in the pons of MSTN patients and their corresponding regions in CTN patients (Fig. 8). Through qualitative analysis, however, the MMs highlighted focal areas of reduced myelin content in the NAWM that were poorly delineated on conventional T1-w and T2-w images in some MSTN patients (Fig. 6). This may suggest that MM can detect modest reductions in myelin within NAWM before a MS plaque is fully formed. Previous studies have also demonstrated the use of MMs to determine changes in the NAWM of MS patients (Beer et al., 2016; Cooper et al., 2019). While our current protocol appears promising in its ability to detect NAWM changes, histopathological correlates are needed to validate this approach in the clinical setting.

4.4. Limitations

One limitation is that MMs are affected by artifacts on the MR images. To mitigate the inclusion of artifacts, we applied a Gaussian curve to capture 99% of the image intensities, thus removing outliers that are within the highest and lowest 0.5% of image intensities for a particular scan. Generating a MM requires two separate scans, rendering it more robust to motion artifacts than one individual scan.

Given its highly sensitive nature, MMs can be affected by non-demyelinating processes. We observed that three patients exhibited temporarily-enlarged PVS, which are cavities containing cerebrospinal fluid in regions surrounding cerebral blood vessels. PVS can be temporarily enlarged in healthy individuals (Maclullich et al., 2004) or permanently enlarged when associated with WM lesions (Fonov et al., 2011; Ontaneda et al., 2017). PVS were visually identified and these MR images were excluded, given the rarity and transient nature of PVS. Previous studies have also demonstrated the effects of edema, inflammation, iron deposition, and dendritic density on T1-w/T2-w ratio maps (Righart et al., 2017; Stüber et al., 2014). The relative contribution of these factors to the T1-w/T2-w ratio maps should be examined in future studies. Future studies should also incorporate MRI with gadolinium to delineate active plaques and investigate MM differences between active and inactive plaques.

In this study, the MM pipeline was applied to MS patients with varying degrees of demyelination, but was not been applied to patients with other diffuse white matter diseases, such as leukodystrophies. Future studies should explore and validate the use of MMs in these patient populations.

4.5. Future steps

The opportunity to create patient-specific MMs allows clinicians to longitudinally and quantitatively assess the degree of disease-related changes *in vivo*, which is particularly valuable in evaluating demyelinating diseases. Capitalizing on routine MR images to predict tissue destruction and patient outcomes holds significant clinical implications. Previous studies have shown that MM intensities can successfully differentiate between MS plaques with varying degrees of demyelination, where relatively preserved myelin content in MSTN patients was associated with adequate pain relief after radiosurgery (Li et al., 2019). Future studies should continue to investigate the correlation between MM intensities and other important clinical outcomes. Lastly, longitudinal MM assessments of plaques, coupled with histological evidence, can help to determine the patterns in MM intensities that are associated with demyelination, remyelination, and dysmyelination in the brain (Klistorner et al., 2016).

CRediT authorship contribution statement

Cathy Meng Fei Li: Conceptualization, Methodology, Visualization. **Powell P.W. Chu:** Conceptualization, Methodology, Visualization. **Peter Shih-Ping Hung:** Methodology. **David Mikulis:** . **Mojgan Hodaie:** Conceptualization, Supervision, Resources.

Declaration of Competing Interest

The authors declare that they have no known competing financial interests or personal relationships that could have appeared to influence the work reported in this paper.

References

Halefoglu, A.M., Yousem, D.M., 2018. Susceptibility weighted imaging: Clinical applications and future directions. World J. Radiol. 10 (4), 30–45. https://doi.org/10.4329/wjr.v10.i4.30.

Kilburg, C., McNally, J.S., de Havenon, A., Taussky, P., Kalani, M.Y.S., Park, M.S., 2017. Advanced imaging in acute ischemic stroke. Neurosurg. Focus 42 (4), 1–8. https://doi.org/10.3171/2017.1.FOCUS16503.

Inglese, M., Petracca, M., 2018. MRI in multiple sclerosis: Clinical and research update. Curr. Opin. Neurol. 31 (3), 249–255. https://doi.org/10.1097/WCO.0000000000000559.

Glasser, M.F., Van Essen, D.C., 2011. Mapping Human Cortical Areas In Vivo Based on Myelin Content as Revealed by T1- and T2-Weighted MRI. J. Neurosci. 31 (32), 11597–11616. https://doi.org/10.1523/JNEUROSCI.2180-11.2011.

Ganzetti, M., Wenderoth, N., Mantini, D., 2014. Whole brain myelin mapping using T1- and T2-weighted MR imaging data. Front. Hum. Neurosci. 8, 671. https://doi.org/10.3389/fnhum.2014.00671.

Gordon, E.M., May, G.J., Nelson, S.M., Oct. 2019. MRI-based measures of intracortical myelin are sensitive to a history of TBI and are associated with functional connectivity. Neuroimage 200, 199–209. https://doi.org/10.1016/j.neuroimage.2019.06.026.

Koenig, S.H., 1991. Cholesterol of myelin is the determinant of gray-white contrast in MRI of brain. Magn. Reson. Med. 20 (2), 285–291.

Barkovich, A.J., 2000. Concepts of Myelin and Myelination in Neuroradiology. Am. J. Neuroradiol. 21 (6), 1099–1109.

Schiffmann, R., 2009. Invited Article : An MRI-based approach to the diagnosis of white matter disorders. Neurology 72 (8), 750–759.

Roy, S., Carass, A., Prince, J.L., 2013. Patched Based Intensity Normalization of Brain MR Images. Proceedings. IEEE Int. Symp. Biomed. Imaging 2013, 342–345. https://doi.org/10.1109/ISBI.2013.6556482.

Shinohara, R.T., Sweeney, E.M., Goldsmith, J., Shiee, N., Mateen, F.J., Calabresi, P.A., Jarso, S., Pham, D.L., Reich, D.S., Crainiceanu, C.M., 2014. Statistical normalization techniques for magnetic resonance imaging. NeuroImage Clin. 6, 9–19. https://doi.org/10.1016/j.nicl.2014.08.008.

Clark, K.A., Woods, R.P., Rottenberg, D.A., Toga, A.W., Mazziotta, J.C., 2006. Impact of acquisition protocols and processing streams on tissue segmentation of T1 weighted MR images. Neuroimage 29 (1), 185–202. https://doi.org/10.1016/j.neuroimage.2005.07.035.

Fang, M., Li, J., Gong, X., Antonio, G., Lee, F., Kwong, W.H., Wai, S.M., Yew, D.T., 2005. Myelination of the pig's brain: A correlated MRI and histological study. NeuroSignals 14 (3), 102–108. https://doi.org/10.1159/000086292.

Fischl, B., Salat, D.H., van der Kouwe, A.J.W., Makris, N., Ségonne, F., Quinn, B.T., Dale, A.M., 2004. Sequence-independent segmentation of magnetic resonance images. Neuroimage 23, S69–S84. https://doi.org/10.1016/j.neuroimage.2004.07.016.

Hagiwara, A., Hori, M., Kamagata, K., Warntjes, M., Matsuyoshi, D., Nakazawa, M., Ueda, R., Andica, C., Koshino, S., Maekawa, T., Irie, R., Takamura, T., Kumamaru, K. K., Abe, O., Aoki, S., 2018. Myelin Measurement: Comparison between Simultaneous Tissue Relaxometry, Magnetization Transfer Saturation Index, and T1w/T2w Ratio Methods. Sci. Rep. 8 (1) https://doi.org/10.1038/s41598-018-28852-6.

M. N. Uddin, T. D. Figley, and C. R. Figley, "Effect of echo time and T2-weighting on GRASE-based T1w/T2w ratio measurements at 3T. Magn. Reson. Imaging. 51. November 2017. 35–43. 2018. doi: 10.1016/j.mri.2018.04.012.

Nyul, L.G., Udupa, J.K., 1999. On Standardizing the MR Image Intensity Scale. Magn. Reson. Med. 42, 1072–1081.

Shah, M., Xiao, Y., Subbanna, N., Francis, S., Arnold, D.L., Collins, D.L., Arbel, T., 2011. Evaluating intensity normalization on MRIs of human brain with multiple sclerosis. Med. Image Anal. 15 (2), 267–282. https://doi.org/10.1016/j.media.2010.12.003.

C. M. F. Li, P. S. P. Hung, P. P. W. Chu, S. Tohyama, M. Hodaie. Trigeminal neuralgia associated with multiple sclerosis: A multimodal assessment of brainstem plaques and response to Gamma Knife radiosurgery. Mult. Scler. J., p. Epub ahead of print. 2019. doi: 10.1177/1352458519886070.

Klistorner, A., Wang, C., Fofanova, V., Barnett, M.H., Yiannikas, C., Parratt, J., You, Y., Graham, S.L., 2016. Diffusivity in multiple sclerosis lesions: At the cutting edge? NeuroImage Clin. 12, 219–226. https://doi.org/10.1016/j.nicl.2016.07.003.

Olesen, J., 2018. Headache Classification Committee of the International Headache Society (IHS) The International Classification of Headache Disorders, 3rd edition. Cephalalgia 38 (1), 1–211. https://doi.org/10.1177/0333102417738202.

Thompson, A.J., Banwell, B.L., Barkhof, F., Carroll, W.M., Coetzee, T., Comi, G., Correale, J., Fazekas, F., Filippi, M., Freedman, M.S., Fujihara, K., Galetta, S.L., Hartung, H.P., Kappos, L., Lublin, F.D., Marrie, R.A., Miller, A.E., Miller, D.H., Montalban, X., Mowry, E.M., Sorensen, P.S., Tintoré, M., Traboulsee, A.L., Trojano, M., Uitdehaag, B.M.J., Vukusic, S., Waubant, E., Weinshenker, B.G., Reingold, S.C., Cohen, J.A., 2018. Diagnosis of multiple sclerosis: 2017 revisions of the McDonald criteria. Lancet Neurol. 17 (2), 162–173. https://doi.org/10.1016/S1474-4422(17)30470-2.

Maclullich, A.M.J., Wardlaw, J.M., Ferguson, K.J., Starr, J.M., Seckl, J.R., Deary, I.J., 2004. Enlarged perivascular spaces are associated with cognitive function in healthy elderly men. J Neurol Neurosurg Psychiatry 75 (11), 1519–1523. https://doi.org/10.1136/jnnp.2003.030858.

Zhang, Y., Brady, M., Smith, S., 2001. Segmentation of brain MR images through a hidden Markov random field model and the expectation-maximization algorithm. IEEE Trans. Med. Imaging 20 (1), 45–57. https://doi.org/10.1109/42.906424.

Avants, B.B., Tustison, N.J., Song, G., Cook, P.A., Klein, A., Gee, C., 2011. A Reproducible Evaluation of ANTs Similarity Metric Performance in Brain Image Registration. Neuroimage 54 (3), 2033–2044. https://doi.org/10.1016/j.neuroimage.2010.09.025.A.

Fonov, V., Evans, A., McKinstry, R., Almli, C., Collins, D., 2009. Unbiased nonlinear average age-appropriate brain templates from birth to adulthood. Neuroimage 47 (Supplement 1), S102.

Fonov, V., Evans, A.C., Botteron, K., Almli, C.R., Mckinstry, R.C., 2011. Unbiased Average Age-Appropriate Atlases for Pediatric Studies. Neuroimage 54 (1), 313–327. https://doi.org/10.1016/j.neuroimage.2010.07.033.Unbiased.

Ontaneda, D., Thompson, A.J., Fox, R.J., Cohen, J.A., 2017. Progressive multiple sclerosis: prospects for disease therapy, repair, and restoration of function. Lancet 389 (10076), 1357–1366. https://doi.org/10.1016/S0140-6736(16)31320-4.

Nakamura, K., Chen, J.T., Ontaneda, D., Fox, R.J., Trapp, B.D., 2017. T1-/T2-weighted ratio differs in demyelinated cortex in multiple sclerosis. Ann. Neurol. 82 (4), 635–639. https://doi.org/10.1002/ana.v82.410.1002/ana.25019.

Righart, R., Biberacher, V., Jonkman, L.E., Klaver, R., Schmidt, P., Buck, D., Berthele, A., Kirschke, J.S., Zimmer, C., Hemmer, B., Geurts, J.J.G., Mühlau, M., 2017. Cortical Pathology in Multiple Sclerosis Detected by the T1/T2-Weighted Ratio from Routine Magnetic Resonance Imaging. Ann. Neurol. 82 (4), 519–529. https://doi.org/10.1002/ana.v82.410.1002/ana.25020.

Arshad, M., Stanley, J.A., Raz, N., 2017. Test-retest reliability and concurrent validity of in vivo myelin content indices: Myelin water fraction and calibrated T1 w/T2 w image ratio. Hum. Brain Mapp. 38 (4), 1780–1790. https://doi.org/10.1002/hbm.23481.

Beer, A., Biberacher, V., Schmidt, P., Righart, R., Buck, D., Berthele, A., Kirschke, J., Zimmer, C., Hemmer, B., Mühlau, M., 2016. Tissue damage within normal appearing white matter in early multiple sclerosis: assessment by the ratio of T1- and T2-weighted MR image intensity. J. Neurol. 263 (8), 1495–1502. https://doi.org/10.1007/s00415-016-8156-6.

Cooper, G., Finke, C., Chien, C., Brandt, A.U., Asseyer, S., Ruprecht, K., Bellmann-Strobl, J., Paul, F., Scheel, M., 2019. Standardization of T1W/T2W ratio improves detection of tissue damage in multiple sclerosis. Front. Neurol. 10 https://doi.org/10.3389/fneur.2019.00334.

Stüber, C., Morawski, M., Schäfer, A., Labadie, C., Wähnert, M., Leuze, C., Streicher, M., Barapatre, N., Reimann, K., Geyer, S., Spemann, D., Turner, R., 2014. Myelin and iron concentration in the human brain: A quantitative study of MRI contrast. Neuroimage 93, 95–106. https://doi.org/10.1016/j.neuroimage.2014.02.026.